

Differential Role of Tissue Factor Pathway Inhibitors 1 and 2 in Melanoma Vasculogenic Mimicry¹

Wolfram Ruf,² Elisabeth A. Seftor, Ramona J. Petrovan, Robert M. Weiss, Lynn M. Gruman, Naira V. Margaryan, Richard E. B. Seftor, Yohei Miyagi, and Mary J. C. Hendrix

Department of Immunology, The Scripps Research Institute, La Jolla, California 92037 [W. R., R. J. P.]; Department of Anatomy and Cell Biology, Holden Comprehensive Cancer Center, University of Iowa, Iowa City, Iowa 52242-1109 [E. A. S., L. M. G., N. V. M., R. E. B. S., M. J. C. H.]; Department of Internal Medicine, Carver College of Medicine, University of Iowa, and Department of Veteran Affairs Medical Center, Iowa City, Iowa 52242 [R. M. W.]; and Kanagawa Cancer Center Hospital and Research Institute, Yokohama, 241-0815 Japan [Y. M.]

ABSTRACT

Vasculogenic mimicry (VM), the formation of matrix-rich vascular-like networks in three-dimensional culture corresponding with the expression of vascular cell-associated genes, and the lining of matrix-rich networks *in situ*, has been observed in highly aggressive and malignant melanoma. However, little is known about the molecular underpinnings of this phenomenon. On the basis of gene profiling, protein detection, and immunohistochemistry, aggressive relative to poorly aggressive melanoma showed up-regulation of tissue factor (TF), TF pathway inhibitor 1 (TFPI-1) and 2 (TFPI-2), critical genes that initiate and regulate the coagulation pathways. The procoagulant function of TF on highly aggressive melanoma is shown to be regulated by TFPI-1 but not by TFPI-2. Thus, aggressive melanoma exhibits endothelial cell-like anticoagulant mechanisms that may contribute to the fluid-conducting potential of melanoma cell-lined networks, as studied by correlative *in vivo* Doppler flow measurements. Antibody inhibition experiments reveal that TFPI-2 is required for VM *in vitro*, but plasmin is an unlikely target protease of TFPI-2. Blockade of TFPI-2 suppressed matrix metalloproteinase-2 activation, and, therefore, TFPI-2 appears to regulate an essential pathway of VM. TFPI-2 is synthesized by endothelial and tumor cells, which deposit TFPI-2 into extracellular matrices. Culturing poorly aggressive melanoma cells on three-dimensional matrix containing recombinant TFPI-2 produces some of the phenotypic changes associated with aggressive, vasculogenic melanoma cells. Thus, TFPI-2 contributes to VM plasticity, whereas TFPI-1 has anticoagulant functions of relevance for perfusion of VM channels formed by TF-expressing melanoma cells.

INTRODUCTION

The gene expression analyses of aggressive cutaneous and uveal melanoma cells revealed that aggressive tumor cells express genes associated with multiple cellular phenotypes (1–3), including genes normally associated with endothelial, epithelial, fibroblast, pericyte, hematopoietic lineage, and several other precursor cell types. These unexpected findings suggest that aggressive melanoma cells might undergo genetic reversion to an undifferentiated, embryonic-like phenotype, indicative of a deregulated cell. On the basis of the molecular profile of aggressive melanoma cells, together with novel *in vitro* observations and correlative histopathologic findings, our laboratory and collaborators introduced the concept of VM³ (4). At the time of its introduction, VM described the unique characteristic of aggressive

melanoma cells to express endothelial-associated genes and form *de novo* ECM-rich vasculogenic-like networks in three-dimensional culture.

These networks had a distinctive pattern that appeared to recapitulate embryonic vasculogenic networks, and correlated with ECM-rich networks observed in the aggressive melanoma tumors of cancer patients, detected by PAS staining (review in Refs. 5, 6). Additional morphological characterization revealed that these networks were rich in laminin, and lined by tumor cells (7) and tightly encircled spheroidal nests of melanoma cells. Most intriguing were the small channel-like spaces among many of the networks, which were originally called “vascular channels” because they were observed to contain plasma and some RBCs. On the basis of these findings, it was tempting to speculate that the channel-like spaces provided a perfusion mechanism within the tumor compartment that functioned either independently of or simultaneously with angiogenesis or vessel co-option, or other sources of vascular supply (4).

Many of the genes overexpressed by aggressive melanoma cells include those involved in angiogenesis and vasculogenesis, such as vascular endothelial cadherin, EphA2 (also called epithelial cell kinase), and laminin 5 γ 2 chain (7–9). These molecules (and their binding partners) have been shown to be critical for the formation and maintenance of blood vessels as well (10–12). Additional experiments focused on the tumor cell-associated ECM that is actively remodeled by aggressive melanoma cells, and contributes to a vasculogenic and more migratory phenotype that involves the cooperative interactions of laminin 5 γ 2 chain with MMPs (7).

Among the other vascular cell-associated genes that are up-regulated by aggressive melanoma are TF, its physiological inhibitor TFPI-1, and a closely related Kunitz-type inhibitor, termed TFPI-2/placental protein 5 (2). TF, structurally related to cytokine receptors, is the initiating cell surface receptor of the coagulation cascade and serves as the cofactor for VIIa (13–15). The complex of TF-VIIa activates coagulation factor X and, thus, triggers hemostasis through downstream thrombin generation, resulting in fibrin formation and platelet activation. The activity of the TF-VIIa complex is physiologically regulated on the endothelium by TFPI-1 (16), which is typically associated with glycosyl-phosphatidyl inositol-anchored receptors on the cell surface (17–19). TFPI-1 consists of three Kunitz-type inhibitory domains and a basic, proteoglycan-binding COOH terminus. TFPI-1 locks TF into an inactive TF-VIIa-Xa-TFPI-1 complex by binding simultaneously to factors VIIa and Xa. TF expression by tumor cells greatly enhances the efficiency of experimental metastasis (20). TF is also involved in vascular development (21) and is induced in angiogenic endothelial cells (22). Up-regulation of TF in angiogenesis leads to a more procoagulant vascular surface, but this shift is balanced by anticoagulant mechanisms, including endothelial cell-expressed TFPI-1, that maintain a patent vascular bed.

TFPI-2 has been identified originally by homology to TFPI-1, as a placental trypsin inhibitor, or as a serine protease inhibitor associated with the ECM of tumor cells (23–25). TFPI-2 associates with the matrix through ionic interactions presumably involving the basic

Received 3/28/03; revised 6/9/03; accepted 6/17/03.

The costs of publication of this article were defrayed in part by the payment of page charges. This article must therefore be hereby marked *advertisement* in accordance with 18 U.S.C. Section 1734 solely to indicate this fact.

¹This work is supported by NIH Grants P01-HL 16411 (to W. R.), CA59702, CA80318, and CA99043-02S (to M. J. C. H.).

²To whom requests for reprints should be addressed, at Department of Immunology, C204, The Scripps Research Institute, 10550 North Torrey Pines Road, La Jolla, CA 92037. Phone: (858) 784-2748; Fax: (858) 784-8480; E-mail: ruf@scripps.edu.

³The abbreviations used are: VM, vasculogenic mimicry; ECM, extracellular matrix; TF, tissue factor; TFPI, tissue factor pathway inhibitor; TFPI-2/K2, tissue factor pathway inhibitor-2 having Kunitz-domain 2 replaced with the homologous domain of tissue factor pathway inhibitor-1; MMP, matrix metalloproteinase; PAS, periodic acid schiff; VIIa, coagulation factor VIIa; CHO, Chinese hamster ovary; RT-PCR, reverse transcription-PCR.

COOH terminus of TFPI-2. Potential binding sites in the matrix are proteoglycans, as well as certain ECM proteins, such as collagen I, vitronectin, and laminin 5 (26). TFPI-2 is a potent inhibitor of plasmin, and, *in vitro*, has some inhibitory activity toward TF-VIIa (27). However, there is no clear evidence that TFPI-2 functionally regulates the TF pathway at physiological levels. Recent evidence suggests that MMPs are also targets for inhibition by TFPI-2 (28, 29), which, in conjunction with the potent inhibitory activity toward plasmin, may account for the anti-invasive and antimigratory effects of TFPI-2 (30–32). However, TFPI-2 expression has also been shown to enhance the migration of certain tumor cells (33), and TFPI-2 is up-regulated on smooth muscle cells with a migratory phenotype (34). In addition, TFPI-2 is synthesized by endothelial cells and supports their firm adhesion by effects that are independent of the inhibition of plasmin (35). These documented diverse effects suggest that matrix-associated TFPI-2 can regulate adhesion and migration of endothelial cells and tumor cells in a context-dependent manner.

The coagulation protease cascade and the fibrinolytic system play important regulatory roles in angiogenesis and tumor growth. Because aggressive melanoma cells express TF *in vitro*, one may expect that the formation of a tumor cell-lined matrix network by these cells precipitates intravascular thrombosis upon conduction or perfusion with blood plasma components, unless effective regulatory mechanisms are in place. Most recent studies have indeed confirmed the presence of a “fluid-conducting meshwork” in melanoma that corresponds to the tumor cell-lined PAS/laminin-positive patterned networks (36, 37), using *i.v.* tracers that demonstrated the conduction of fluid. *In situ*, this fluid-conducting meshwork has been shown to contain fibrinogen (37), indicative of plasma, in addition to some RBCs, likely to be derived from local tumor vasculature that is leaky and undergoing remodeling. In addition, *i.v.*-injected phage has been shown to rapidly localize to tumor cell-lined channels in prostate cancer (38), and breast cancer imaging studies (39, 40) reported the *in vivo* perfusion of VM channels.

In the present study, we examined the potential role(s) of overexpressed coagulation pathway molecules, and found that aggressive melanoma cells *in vivo* express TF, TFPI-1, and TFPI-2 in concordance with gene profiling experiments. TFPI-1, but not TFPI-2, is shown to serve as the predominant regulator of TF function in aggressive melanoma cells, thus endowing them with the same regulatory capability as endothelial cells. TFPI-2 is shown to play a crucial role in the formation of vasculogenic-like networks by aggressive melanoma cells. Blocking antibodies to TFPI-2 prevented network formation, and TFPI-2 associated with a three-dimensional collagen matrix can induce the VM phenotype in poorly aggressive melanoma cells. Thus, these experiments demonstrate a novel function of TFPI-2 in melanoma VM.

MATERIALS AND METHODS

Proteins and Antibodies. Recombinant VIIa and plasma-derived factor X were as described (41). Active site-blocked VIIa was generated by reacting recombinant VIIa with Phe-Phe-Arg chlormethyl ketone, as described (42). Recombinant human TFPI-1 was kindly provided by Dr. Abla Creasy (Chiron Corporation, Emeryville, CA), and human plasmin was purchased from Hematological Technologies (Essex Junction, VT). Polyclonal antibodies to recombinant TFPI-1, TFPI-2 (R6167), and VIIa were raised by repeated immunizations of rabbits, and prepared and purified by ammonium sulfate precipitation and DEAE Sephacel chromatography of the IgG fractions. Antibody R1552 to TFPI-2 was generated by repeated immunization with naked DNA, as described (43). Both R1552 and R6167 recognized preferentially native TFPI-2. For Western blotting of reduced TFPI-2, the antibody described previously (44) raised against a glutathione *S*-transferase-TFPI-2 fusion protein was used. An inhibitory mixture of monoclonal antibodies against TF

contained TF8–5G9, TF9–5B7, and TF9–9C3 to nonoverlapping epitopes in TF (45, 46).

Constructs for *Escherichia coli* expression of TFPI-2 were generated by cloning of the TFPI-2 coding sequence (starting with Ala; Ref. 20) of the mature NH₂ terminus of TFPI-2) in frame after hexa-His sequence of pQE-80L (Qiagen, Valencia, CA) into the *Bam*HI site. The TFPI-2/K2 chimera was constructed by replacing the TFPI-2 Kunitz domain 2 (23) with the corresponding domain of TFPI-1 (47), followed by subcloning into the *Bam*HI/*Pst*I-restricted TFPI-2/pQE-80L. Recombinant protein was expressed in M15 cells (Qiagen), and inclusion bodies were isolated (48). Inclusion bodies were resuspended by sonication in 12 ml of 6 M guanidine, 0.5 M NaCl, 20 mM K/sodium phosphate, 10 mM β -mercaptoethanol, and protease inhibitor mixture (Roche, Indianapolis, IN; pH 8.0), and insoluble protein was removed by centrifugation after overnight incubation at ambient temperature. TFPI-2 was refolded by diluting the solubilized inclusion bodies to a concentration of 0.4 g/liter into 20 mM Tris (pH 8.0), 6 M urea, 0.3 M NaCl, 0.01% Brij-35, and 2 mM L-Cysteine, as described by Rao *et al.* (32). After incubation at ambient temperature overnight, the solution was diluted 1:2 with water, kept overnight at ambient temperature, and then additionally incubated for 2–3 weeks at 4°C to complete the folding. Refolded recombinant TFPI-2 solution was adjusted to 20 mM imidazole, adsorbed to Ni-NTA agarose, and eluted with 20 mM Tris (pH 8.0), 1 M urea, and 250 mM imidazole. Eluted protein was adjusted to 1 M NaCl (pH 5.0) and dialyzed against the storage buffer [0.1 M Na-Acetate (pH 4.5) and 0.1 M NaCl]. Proper folding of recombinant TFPI-2 was confirmed by inhibition of plasmin activity. Plasmin (5 nM) was incubated with up to 250 nM of TFPI-2 or TFPI-2/K2 in HEPES buffer saline (HBS) [10 mM HEPES, and 150 mM NaCl (pH 7.4)], 5 mM CaCl₂, and 0.2% BSA. Residual plasmin activity was determined from hydrolysis of the chromogenic substrate S-2366 (Chromogenix) in a kinetic microtiter plate reader. To analyze the effect of antibodies on inhibition of plasmin by TFPI-2, 2 μ M of antibody were preincubated with TFPI-2 preparations for 15 min before the addition of plasmin.

Cell Culture. The human cutaneous (C81–61 and C8161) and uveal (MUM-2C and MUM-2B) melanoma cells have been described previously (9), and except for the C81–61 cells, were maintained in RPMI 1640 (Invitrogen Life Technologies, Inc., Carlsbad, CA) supplemented with 10% fetal bovine serum and 0.1% gentamicin sulfate (Gemini Bioproducts, Calabasas, CA). The C81–61 cells were maintained in Ham’s F10 medium (Invitrogen) supplemented with 15% fetal bovine serum, 1 \times MITO+ (BD Biosciences, Bedford, MA), and 0.1% gentamicin sulfate. Cell cultures were determined to be free of *Mycoplasma* contamination using a PCR-based ELISA detection assay (Roche).

Three-dimensional type I collagen gels were produced as follows: 25 μ l of type I collagen (average 3 mg/ml; BD Bioscience) were dropped onto 18-mm glass coverslips in 12-well culture dishes and polymerized with an application of 100% ethanol for 5 min at room temperature. After a wash with PBS, tumor cells were seeded onto the three-dimensional matrix in complete medium. For experiments designed to analyze the matrix after preconditioning by the aggressive MUM-2B cells, the cells were removed after 3 days with 20 mM NH₄OH followed by three quick washes with water. For experiments using blocking antibodies or inhibitors, aggressive C8161 or MUM-2B cells were seeded onto the three-dimensional matrix for 4 days in the presence or absence of the agent added to the culture fresh each day (50–100 μ g/ml). Experiments with preconditioned matrices treated with anti-TFPI-2 were performed as follows: matrices were preconditioned by the aggressive MUM-2B or C8161 cells as described above. After removing the cells and washing, the matrix was incubated with either 1 \times PBS (control) or TFPI-2 antibody (R1552; 100 μ g/ml) overnight at 37°C. The matrix was then washed once with 1 \times PBS and seeded with the poorly aggressive MUM-2C or C81–61 cells in complete medium.

Immunohistochemistry. Formalin-fixed, paraffin-embedded melanoma tumors were derived from patient uveal melanoma samples or human cutaneous melanoma xenografts (formed by C8161 aggressive tumor cells) from nude mice ($n = 6$). All of the patient samples were collected in compliance with requirements of the Institutional Review Board for the Protection of Human Subjects. Two nevus-like, spindle cell type, poorly aggressive choroidal melanoma and two epithelioid cell type, aggressive choroidal melanoma were used in this study. The tumor tissues were sectioned at 4 μ m and stained with either H&E or PAS without hematoxylin. Adjacent sections were stained with polyclonal antibodies directed against TF (1:1000 dilution), TFPI-1

(R3648; 1:400 dilution), or TFPI-2 (R1552; 1:90 dilution) and RTU Vectastain Universal Elite ABC Peroxidase kit (Vector Laboratories, Burlingame, CA) in a Dako Autostainer (Dako, Carpinteria, CA) as per the manufacturer's protocol. Color for the RTU procedure was produced by using 3,3'-diaminobenzidine + (brown) Substrate (Dako) for 2–3 min. Slides were counterstained with Mayer's Hematoxylin (Dako) for 3 min.

Color Doppler Ultrasound and Microbubble Imaging. Nude mice bearing tumor xenografts of aggressive human cutaneous melanoma tumors (formed by C8161 cells) were sedated with midazolam, 0.3 mg s.c., which renders them sentient and ambulatory, but docile. The tumor region was localized by palpation. Mice were gently grasped by the nape of the neck and cradled in the operator's left hand. Prewarmed acoustic coupling gel was applied in abundance so as to effect a 2–4-mm "stand-off." Two-dimensional images were obtained by gentle application of a 15 MHz linear array transducer (Acouson/Siemens, Issaquah, WA), yielding 166 frames/second. A subset of melanoma-bearing mice ($n = 4$) underwent induction of general anesthesia (pentobarbital, 50 mg/kg i.p.), followed by catheterization using a PE10 polyethylene tubing (Becton Dickinson, Sparks, MD) in the proximal aorta via carotid cutdown. A bolus of 0.15 ml of gas-filled albumin-coated microspheres (Optison[®]; nominal diameter = 3–4 μ m) was injected during continuous two-dimensional imaging to ascertain the distribution of tumor perfusion at the microvascular level.

Western Blot Analysis. Samples for Western blot analysis were prepared as follows. Cells were grown on three-dimensional collagen I matrices for 4 days and the denuded matrix prepared as described above. The matrix was then scrapped into Laemmli sample buffer, sonicated (in pulses) for 3 s, then microfluided at 4°C for 30 min at 13,000 rpm. Matrix extracts were separated on 4–16% SDS-PAGE gels and analyzed by Western blot analysis after semidry blot transfer, using an anti-TFPI-2 antibody with strong reactivity with denatured protein, as described (44). To detect total cellular expression of TF, TFPI-1, or TFPI-2, cells grown on plastic or collagen matrix were directly lysed in reducing sample buffer, sonicated, and analyzed by Western blotting using monospecific, polyclonal antibodies.

Factor Xa Generation Assay. To characterize TF procoagulant activity of melanoma cells *in vitro*, cells were seeded on 12-well plates on plastic or three-dimensional collagen matrix and grown to confluence. Wells were washed with cell buffer [21 mM HEPES, 137 mM NaCl, 5 mM KCl, 0.75 mM Na₂HPO₄, and 5.5 mM glucose (pH 7.4)], 2 mM CaCl₂, and preincubated for 10 min with anti-TFPI-1 or TFPI-2 antibody (50 μ g/ml). VIIa (10 nM) and factor X (50 nM) were then added to measure the rate of factor Xa generation by chromogenic assay. To test the inhibitory activity of TFPI-1, TFPI-2, or TFPI-2/K2, TF-expressing CHO-K1 cells (20) were preincubated in cell buffer with the indicated concentrations of inhibitor for 15 min, followed by addition of VIIa and factor X to determine TF activity, as above.

Measurement of MMP Protein and Endogenously Active Protein Concentrations. Measurement of the protein concentration of pro-MMP-2 (including pro-MMP-2 bound to tissue inhibitor of metalloproteinase-2) and endogenously active MMP-2 in response to the different antibody treatment regimen were made using the Biotrak Cellular Communication Assays from Amersham Pharmacia Biotech (Buckinghamshire, England) as per the manufacturer's protocols.

Semiquantitative RT-PCR Analysis. Total RNA from MUM-2C and MUM-2B melanoma cell lines (TRIzol reagent; Invitrogen) was reverse transcribed using the Advantage PCR kit as per the manufacturer's instructions (Clontech Laboratories, Palo Alto, CA). PCR amplifications were performed with gene-specific primers in a Robocycler gradient 96 thermocycler (Stratagene, La Jolla, CA): 1 cycle: 94°C, 1 min; 27–40 cycles: 94°C, 1 min; 60–70°C, 2.5 min, 72°C, 1 min; and 1 cycle: 72°C, 5 min with glyceraldehyde-3-phosphate dehydrogenase primers (Clontech) used as controls for PCR amplification. PCR fragments were ligated into the pCR2.1-TOPO sequencing vector as per the manufacturer's instructions (Invitrogen), and the plasmid DNA isolated and subjected to DNA sequencing analysis using fluorescent Sanger-based dideoxy sequencing on an ABI 373A Automated Sequencer (University of Iowa DNA Facility). Two plasmids from each primer set were sequenced and shown to contain 100% identity to the expected DNA sequence.

Microarray Analysis. Microarray analyses of MUM-2B compared with MUM-2C melanoma cell lines were performed using the U133A Human Genome Array from Affymetrix (Santa Clara, CA) by the University of Iowa DNA Facility. The raw data were collected and analyzed by using Affymetrix

Microarray Suite and Data Mining Tools software. For comparison of multiple samples, average difference values from each individual chip were scaled such that the average intensity of any given chip was 1500.

RESULTS

Expression of TF, TFPI-1, and TFPI-2 by Aggressive Melanoma *in Vivo*. Genome-wide expression profiling of tumor cell populations with different levels of aggressiveness has provided evidence for the up-regulation of a set of genes that indicate a pluripotent, embryonic-like genotype in highly aggressive uveal melanoma MUM-2B cells in comparison to poorly aggressive MUM-2C cells (2). MUM-2B cells showed increased mRNA levels of TF, TFPI-1, and TFPI-2 in comparison to MUM-2C cells, but the liver-synthesized plasma coagulation factors X and VII were not expressed by melanoma cells (Table 1). To confirm the relevance of these findings in uveal melanoma, protein expression was characterized by immunohistochemistry in clinical samples (Fig. 1). PAS staining revealed the presence of ECM-rich patterned networks (a fluid-conducting meshwork; Refs. 36, 37) surrounding spheroidal nests of melanoma cells in the aggressive tumors, but not in the poorly aggressive tumors (Fig. 1, A and B). TF was expressed throughout aggressive uveal melanoma, including channel-like areas where RBCs were observed in close contact with melanoma cells (Fig. 1C), but TF was absent in poorly aggressive tumors (Fig. 1D). We have found previously in bladder carcinoma that the physiological ligand of TF, coagulation factor VIIa, colocalizes with TF, suggesting extravasation of VIIa from the blood plasma and association with tumor cell expressed TF (43). Aggressive, but not the poorly aggressive, melanoma cells stained positive for VIIa (data not shown), additionally supporting a close contact of aggressive tumor cells with the circulatory system *in vivo*. In addition, aggressive melanoma stained strongly for TFPI-1 (Fig. 1E) and TFPI-2 (Fig. 1G), but these inhibitors were not appreciably expressed by the poorly aggressive tumors except in the endothelial-lined vasculature (Fig. 1, F and H). Whereas the staining pattern for TFPI-2 appeared more intense than TFPI-1 throughout the aggressive melanoma tissue samples, the pattern of staining for TFPI-1 and TFPI-2 (Fig. 1, E and G) was remarkably prominent along the tumor cell-lined matrix-rich extravascular networks (comprising a fluid-conducting meshwork) encasing spheroidal nests of melanoma tumor cells. Thus, the expression of TF, TFPI-1, and TFPI-2 by aggressive melanoma *in vivo* confirms the *in vitro* gene profiling data that demonstrated an up-regulation of these genes in aggressive uveal melanoma cell lines.

TFPI-1 Is the Major Inhibitor of the TF Coagulation Pathway in Aggressive Melanoma Cells. It has been documented for several tumor types that tumor cell TF triggers blood coagulation, leading to extravascular fibrin deposition in the tumor stroma (49). Angiogenic endothelial cells also express TF (22), but excessive intravascular fibrin deposition and occlusive thrombosis is typically not observed in the tumor vasculature, reflecting either high fibrinolytic potential

Table 1 Molecular analysis of melanoma cells

Gene	Mean fold difference ^a
TF	↑ 39.0
TFPI-1	↑ 8.6
TFPI-2	↑ >100
Factor VII	absent ^b
Factor X	absent
MMP-2	↑ 9.9
MMP-14 (MT1-MMP)	↑ 5.3

^a Mean fold increase in expression of aggressive compared to poorly aggressive melanoma tumor cells assessed by Affymetrix oligonucleotide gene chip arrays.

^b Analysis determined that this gene is not expressed (absent) by either aggressive or poorly aggressive melanoma tumor cells.

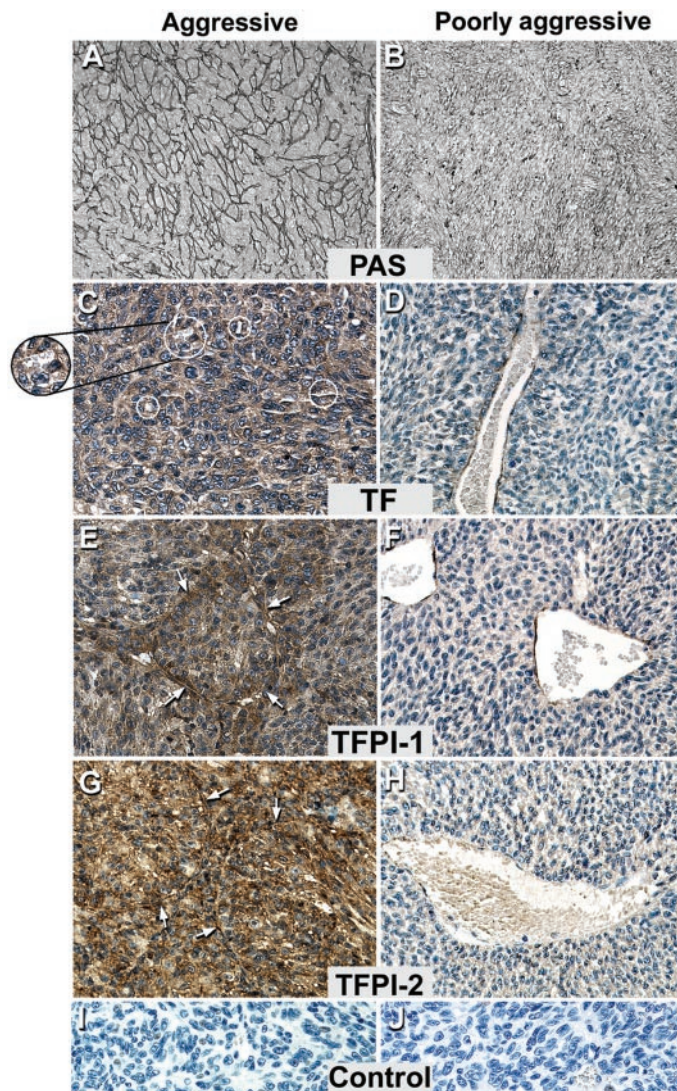


Fig. 1. Light microscopy of histological sections of uveal melanoma patient tumors, classified as aggressive (with predominantly epithelioid cell type; A, C, E, G, and I) or poorly aggressive (with predominantly spindle cell type; B, D, F, H, and J) stained with PAS or for different coagulation markers. A, PAS-stained aggressive melanoma reveals patterned, ECM-rich networks, characteristic of melanoma VM. B, PAS-stained poorly aggressive melanoma shows no patterned ECM-rich networks. C, TF staining is intensely distributed throughout aggressive melanoma cells (magnified circle showing unstained, translucent RBCs in a tumor cell-lined channel-like space), but primarily found along the endothelial-lined vasculature (D) in poorly aggressive melanoma. E, TFPI-1 staining is strongest in the aggressive melanoma cells, particularly lining patterned ECM-rich networks (arrows), and in the vascular endothelia of poorly aggressive melanoma (F). G, intense TFPI-2 staining is shown throughout aggressive melanoma including along tumor cell-lined networks (arrows), compared with poorly aggressive (H) melanoma where TFPI-2 is found in the endothelia of the vasculature. Aggressive (I) or (J) poorly aggressive melanoma, respectively, treated with secondary antibody only (control), shows no nonspecific staining (original magnification $\times 100$, A and B; $\times 400$, C–J).

and/or effective anticoagulant mechanisms. Because extravascular channels of TF-expressing tumor cells are expected to trigger blood coagulation upon exposure to blood plasma, we analyzed whether aggressive tumor cell TF is functionally regulated by the cell-associated inhibitors TFPI-1 and TFPI-2.

Fig. 2A shows the expression of TF, TFPI-1, and TFPI-2 by matching pairs of aggressive and poorly aggressive uveal (MUM-2B versus MUM-2C) or cutaneous (C8161 versus C81–61) melanoma cells, respectively, *in vitro*. Similar to uveal melanoma, cutaneous melanoma showed a concordant up-regulation of TF and TFPI-2 in aggressive, but not in the poorly aggressive, cell counterparts. Aggressive cells expressed cell-associated TFPI-1, but TFPI-1 protein

was also detectable in the poorly aggressive MUM-2C uveal melanoma cells. TFPI-1 mRNA levels were clearly different between MUM-2B and MUM-2C cells (Table 1), indicating that TFPI-1 protein levels may be regulated by additional post-transcriptional mechanisms resulting in the observed levels of cell-associated TFPI-1. Aggressive melanoma cells spontaneously form VM network structures when cultured on three-dimensional collagen. Collagen culture did not change the expression patterns of TF, TFPI-1, or TFPI-2 (Fig. 2A, right panel). Cell-associated TFPI-1 is known to rapidly down-regulate TF proteolytic activity on cultured cells *in vitro*. Inhibitory antibodies to TFPI-1 typically increase TF procoagulant activity of TFPI-1-expressing cells (19, 44). Fig. 2B shows that the rate of factor Xa generation, a measure of the procoagulant function of the TF-VIIa complex, is accelerated 2-fold in the presence of inhibitory anti-TFPI-1 antibodies. TF-transfected CHO-K1 cells do not express TFPI-1, and no effect of the inhibitory antibody was observed in these controls. Thus, TFPI-1 is a relevant inhibitor of the procoagulant activity of TF on aggressive melanoma cells.

Blood Flow in Aggressive Human Melanoma Xenografts. The finding that aggressive melanoma cells have anticoagulant properties similar to endothelial cells prompted us to analyze whether tumor cell-lined extravascular networks are perfused *in vivo*. Doppler imaging was used to study the blood flow in aggressive human melanoma xenografts, with special focus on the endothelial-lined vasculature at the tumor periphery and the tumor cell-lined channel-like spaces that appear extravascular (Fig. 3, A and B). Color Doppler reveals abundant turbulent flow at the tumor rim (Fig. 3C, panel 1; during diastole) that corresponds to the mouse endothelial-lined neovasculature shown in Fig. 3A. In-flow to the central region of the tumor was visible only

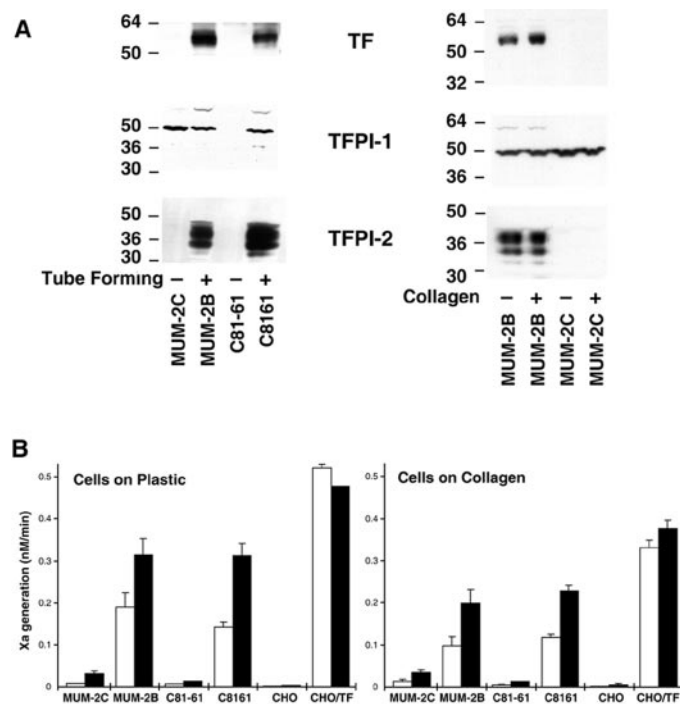


Fig. 2. Expression of extrinsic coagulation components by aggressive and poorly aggressive melanoma cells. A, Western blot analysis of protein expression of TF, TFPI-1, and TFPI-2. Cells were grown to confluence either on plastic or three-dimensional collagen and lysed with reducing sample buffer added to the wells. The left panel shows the comparison of aggressive and poorly aggressive uveal (MUM-2B and MUM-2C) and cutaneous (C8161 and C81–61) melanoma cells; the right panel shows the effect of three-dimensional collagen culturing on protein expression of uveal melanoma cells. B, TF procoagulant activity of melanoma clones grown on plastic or collagen for 3 days. Factor Xa generation was determined in the absence (□) or presence (■) of 50 $\mu\text{g/ml}$ α -TFPI-1 antibody in an end point assay after 2 min at 37°C (mean SD; $n = 3$).

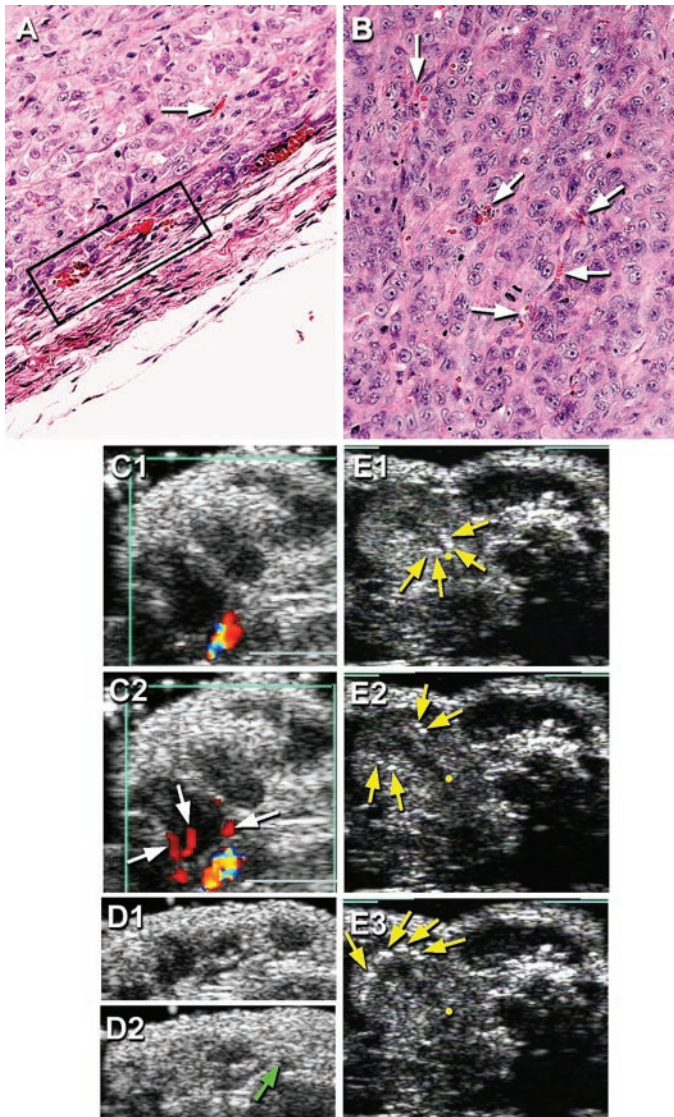


Fig. 3. Two-dimensional ultrasound and color Doppler imaging (with H&E photomicroscopy orientation) of blood flow with microbubbles in aggressive human cutaneous melanoma xenografts from a nude mouse. H&E-stained histological sections from (A) tumor rim (mouse-human tissue interface) and (B) tumor core. White arrows depict deformed erythrocytes within channel-like spaces lined by tumor cells. C1, diastolic and (C2) systolic color Doppler images. Abundant turbulent (multicolor) flow persists at the tumor rim (C1, corresponding to black rectangular area shown in A), whereas in-flow to tumor center (red; C2) is visible only during systole. Two-dimensional images before (D1) and after (D2) systemic arterial injection of microbubbles. Homogeneous tumor opacification by perfused microbubbles (green arrow) is complete in <200 ms (2 cardiac cycles). E1–E3, serial two-dimensional images depicting arrival of microbubbles within the tumor core. (Yellow arrows show progress of microbubbles through series beginning at the yellow point of reference.)

during systole (Fig. 3C, panel 2) and corresponds to the tumor cell-lined extravascular channel-like spaces shown in Fig. 3B. Two-dimensional imaging within the central region of the tumor before (Fig. 3D, panel 1) and after (Fig. 3D, panel 2) the arterial injection of microbubbles showed that homogeneous tumor opacification by the perfused microbubbles was completed in <200 ms (2 cardiac cycles). Additional tracking of these microbubbles is shown in serial two-dimensional images (Fig. 3E, panels 1–3), and indicates a connection between the arterial vasculature and the tumor cell-lined extravascular pathway. A video corresponding to Fig. 3 C1–C2, D1–D2 and E1–E3 is available.⁴

⁴ Internet address: http://www.anatomy.uiowa.edu/hendrix_nat.rev.cancer/.

TFPI-2 Does Not Regulate TF Procoagulant Activity of Aggressive Melanoma Cells. Whether TFPI-2 is a relevant inhibitor to regulate the functional activity of the TF-VIIa complex was analyzed by antibody blocking experiments and by using recombinant, purified TFPI-2. TFPI-2 is highly homologous to TFPI-1 and inhibits plasmin and, less potently, TF-VIIa through the first Kunitz inhibitory domain. However, unlike TFPI-1, the Kunitz domain 2 of TFPI-2 does not inhibit factor Xa, and the linker regions between Kunitz domain 2 and domain 1 or 3 are significantly shorter in TFPI-2, as compared with TFPI-1. A mutant of TFPI-2 was generated that replaces Kunitz domain 2 with the homologous domain of TFPI-1, whereas maintaining the original linker length of TFPI-2. Recombinant TFPI-2 and TFPI-2/K2 chimera were expressed in *E. coli* and refolded. Both recombinant molecules potently inhibited plasmin, demonstrating that Kunitz domain 1 is properly folded (Fig. 4A). We generated polyclonal rabbit antibodies to TFPI-2 by either naked DNA immunization (antibody R1552; Ref. 43) or by immunization with recombinant *E. coli*-expressed TFPI-2 that lacks the complex carbohydrate composition of TFPI-2 synthesized by eukaryotic cells (antibody R6167). Antibody R6167 potently reversed the inhibition of plasmin activity by TFPI-2 (Fig. 4A), whereas antibody R1552 was a less potent inhibitor of this function of Kunitz domain 1 of TFPI-2 (~60% maximal inhibition at identical antibody concentration; data not shown). Notably, an antibody to TFPI-1 reversed the inhibition of

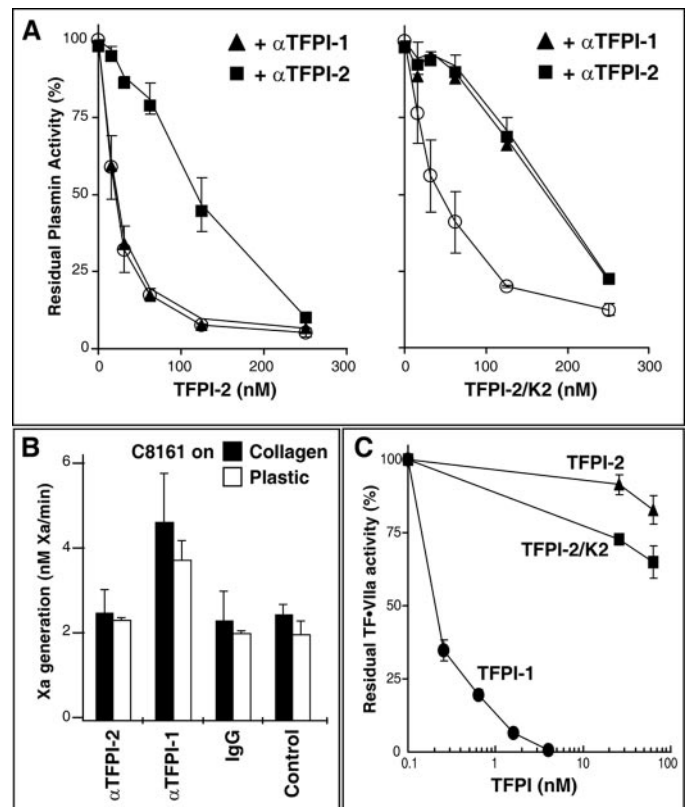


Fig. 4. Role of TFPI-2 in regulating TF procoagulant function on aggressive melanoma cells. A, inhibition of plasmin activity by recombinant TFPI-2 or TFPI-2/K2 chimera demonstrates proper folding and activity of the recombinant protein. Plasmin inhibitory activity is reversed by anti-TFPI-2 (R6167). Anti-TFPI-1 selectively reverses the inhibitory activity of TFPI-2/K2 chimera, consistent with binding to a properly folded Kunitz domain 2 of TFPI-1 in the recombinant protein. B, anti-TFPI-2 (R6167) does not increase TF procoagulant activity of C8161 aggressive melanoma cells whether cells were cultured on plastic or collagen. Cells were incubated in serum-free medium overnight with 50 μ g/ml of antibody, and factor Xa generation was determined after addition of VIIa/factor X for 10 min at 37°C. C In comparison to TFPI-1, TFPI-2 or TFPI-2/K2 were weak inhibitors of TF. TF-expressing CHO-K1 cells were preincubated with the indicated concentrations of TFPI, TFPI-2, or TFPI-2/K2. After addition of VIIa/factor X for 15 min at 37°C, factor Xa generation was determined (bars, \pm SD; n = 3).

plasmin by the TFPI-2/K2 chimera, but not by wild-type TFPI-2 (Fig. 4A). The functional inhibition of the chimeric molecule is evidence for binding to the second, TFPI-1-derived Kunitz-domain, implying proper folding of chimera.

TF-VIIa can be inhibited by Kunitz domain 1 of TFPI-2 under certain *in vitro* conditions (50). Unlike inhibitory anti-TFPI-1 antibody, neither the more potent antibody R6167 (Fig. 4B) nor antibody R1552 (data not shown) enhanced TF activity on aggressive melanoma cells, whether cells were grown on plastic or three-dimensional collagen. The role of TFPI-2 in regulating TF proteolytic function was additionally tested with recombinant proteins on TF-expressing CHO-K1 cells that lack endogenous TFPI-1 and TFPI-2 activity (Fig. 4C). On these cells, recombinant TFPI-1 was a potent inhibitor of TF function, and only marginal inhibition of TF function was seen at >10-fold higher concentrations of TFPI-2. The Kunitz domain 2 exchange mutant of TFPI-2 also inhibited TF procoagulant activity poorly, suggesting that the linker length between the Kunitz domains is an additional critical factor for inhibition of the TF-VIIa-Xa complex. Thus, TFPI-1 is the predominant inhibitor of the procoagulant activity of aggressive melanoma cells.

TFPI-2 Is Necessary for VM by Aggressive Melanoma Cells.

Aggressive melanoma cells form vasculogenic-like networks upon culture on three-dimensional collagen. The role of TF, TFPI-1, and TFPI-2 in VM was evaluated by antibody blocking experiments. Polyclonal antibodies to VIIa, a mixture of monoclonal antibodies that completely block the procoagulant function of TF, and active site-inhibited VIIa (VIIai), which is a high-affinity inactive ligand for TF, did not suppress the network formation by aggressive MUM-2B and C8161 melanoma cells (Fig. 5). This indicates that the coagulant or protease signaling functions (15) of TF are not required for the formation of VM network structures *in vitro*. There was a slight delay in the appearance of VM networks when cells were cultured with anti-TFPI-1 or anti-TFPI-2 antibody (R6167). However, anti-TFPI-2 antibody R1552 completely suppressed VM network formation of aggressive melanoma cells. The suppression of these VM networks by antibody R1552 was reversed by recombinant TFPI-2, demonstrating antigen specificity. To test whether TFPI-2 supports VM network formation by inhibiting plasmin activity, the effect of aprotinin, a potent Kunitz-type inhibitor of plasmin, on the inhibition by antibody R1552 was tested. Unlike recombinant TFPI-2, aprotinin did not reverse the suppression of VM network formation by antibody R1552. Plasmin as the target protease for TFPI-2 is also considered unlikely from the inhibitory profile of the two anti-TFPI-2 antibodies that were used in this study. In comparison to antibody R1552, anti-TFPI-2 antibody R6167 more potently reversed plasmin inhibition by TFPI-2, but R6167 was a poor inhibitor of VM network formation.

TFPI-2 is known to bind to ECMs (26). TFPI-2 was found to be deposited into the three-dimensional collagen matrix by aggressive melanoma cells, but no TFPI-2 was detectable in the matrix of poorly aggressive cells (Fig. 6A). Our recombinant TFPI-2 preparation also bound in a dose-dependent manner to collagen I matrix (Fig. 6B), consistent with matrix-binding properties of TFPI-2 described previously (26). Because angiogenic endothelial cells synthesize TFPI-2 (51), we wanted to evaluate whether matrix-associated TFPI-2 has an effect on the plasticity of poorly aggressive melanoma cells. TFPI-2 (Fig. 6C) or TFPI-2/K2 (Fig. 6D) added to three-dimensional-collagen matrix induced morphological changes, but not complete VM network formation in poorly aggressive melanoma cells. To test whether the morphological changes were related to the VM phenotype, we analyzed mRNA levels of TF, TFPI-1, and TFPI-2 that were found to be up-regulated in aggressive *versus* poorly aggressive melanoma cells. When poorly aggressive cells were grown on collagen matrix supplemented with recombinant TFPI-2 or TFPI-2/K2, up-regulation of TF

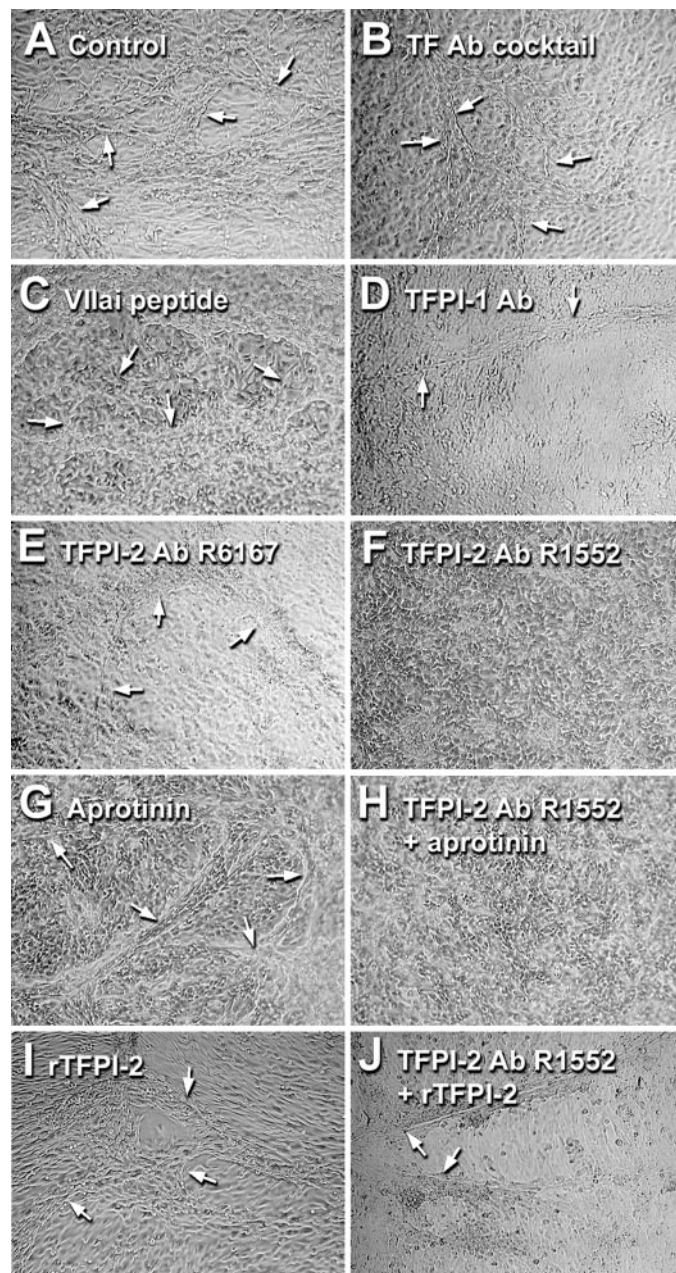


Fig. 5. Phase contrast microscopy showing VM by aggressive C8161 human cutaneous melanoma cells cultured on a three-dimensional collagen I matrix, with or without blocking antibodies to different TFPIs or TF, with the TF inhibitor VIIai, or with aprotinin. A, C8161 cells cultured on a three-dimensional collagen I matrix for 4 days formed patterned, ECM-rich, vasculogenic-like networks (Control), highlighted with white arrows. B, treatment with a mixture of blocking antibodies to TF. C, active site blocked VIIai, G aprotinin, or I rTFPI-2 did not inhibit VM (patterns highlighted with white arrows). Whereas a blocking antibody (D) to TFPI-1 or (E) TFPI-2 (R6167) retarded the establishment of networks, the complete inhibition of network formation F by a different blocking antibody to TFPI-2 (R1552) could be partially reversed (J) by also adding rTFPI-2 to the culture, but not by addition of aprotinin (H; original magnification $\times 100$).

and TFPI-1, but not of TFPI-2, was observed (Fig. 6E). These data may suggest that the VM phenotype is not solely programmed by a genetic master switch, but rather has plasticity that is under control of ECM-derived cues.

MMP activity is crucial for the induction of VM network formation by poorly aggressive melanoma cells on matrices preconditioned by aggressive tumor cells (7, 52). The effect of anti-TFPI-2 (R1552) treatment on MMP-2 secretion and activation of aggressive melanoma

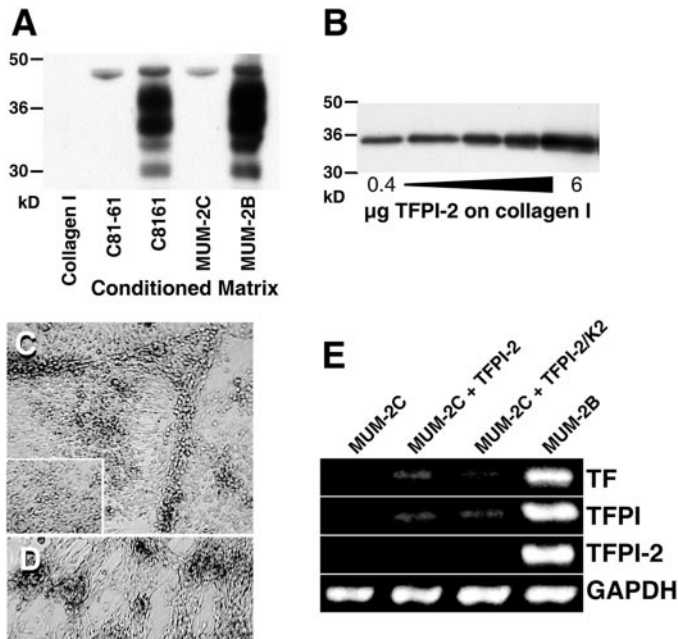


Fig. 6. Effect of matrix-associated TFPI-2 on the phenotype of poorly aggressive melanoma cells. **A**, Western blot analysis of a three-dimensional collagen I matrix preconditioned by aggressive (C8161 or MUM-2B) or poorly aggressive (C81-61 or MUM-2C) melanoma cells, after their subsequent removal, shows the presence of TFPI-2 in the matrix preconditioned by the aggressive cell lines only. **B**, the indicated amount of recombinant TFPI-2 was added to collagen I matrix overlaid with 1 ml of standard tissue culture medium. After 3 days, the matrix was extracted and analyzed by Western blotting as in **A**. The blot shows that recombinant TFPI-2 is bound to the matrix and does not degrade under tissue culture conditions. **C** and **D**, poorly aggressive MUM-2C melanoma cells cultured on a three-dimensional matrix with the addition of (C) rTFPI-2 or (D) TFPI-2/K2. Compare the morphological changes with (inset) MUM-2C cells on a non-preconditioned three-dimensional collagen I matrix forming no networks. **E**, RT-PCR shows the induction of TF and TFPI-1, but not of TFPI-2, mRNA expression in poorly aggressive MUM-2C cells grown on three-dimensional collagen I matrix in the presence of TFPI-2 or the TFPI-2/K2 mutant.

cells grown on three-dimensional collagen was analyzed. Anti-TFPI-1 polyclonal antibody, which was prepared identically as the anti-TFPI-2 antibody, as well as a monoclonal antibody mixture against TF were used as controls. Cells were treated by addition of 50 µg/ml antibody/day for 3 days, followed by harvest of the cell supernatant for determination MMP-2 antigen and endogenous activity (Table 2). All three of the antibodies produced a minor reduction in the antigen levels of MMP-2. In contrast, MMP-2 endogenous activity was reduced 2-fold upon treatment with anti-TFPI-2 (R1552), but essentially unchanged upon treatment with antibodies that did not inhibit VM network formation under these experimental conditions. These data suggest a positive regulatory role of TFPI-2 in the activation of MMP-2 in aggressive melanoma cells.

DISCUSSION

Individuals with melanomas that exhibit VM have a poor prognosis (5), yet little is known about the biological relevance of this phenomenon. Interestingly, VM has been reported in other tumor types, including breast, lung, prostatic, and ovarian carcinoma (38, 53–57) with clinical correlations made to tumor progression. However, one of the most intriguing aspects of VM involves the apparent dysregulation of the tumor-specific phenotype and the concomitant transdifferentiation of aggressive tumor cells to acquire phenotypic markers of other cell types, such as endothelial cells. Thus, the focus of the current study was to address key molecular events that initiate and regulate coagulation pathways in melanoma tumor cells, normally associated with endothelial cells.

The up-regulation of TF concordant with other genes that characterize the unique vasculogenic phenotype of aggressive melanoma raises an important question regarding its biological relevance in aggressive tumors. All of the TF-positive aggressive cells tested in the current study also expressed TFPI-1, and the data revealed that TFPI-1, but not TFPI-2, serves as the relevant inhibitor of TF procoagulant function on VM melanoma cells. Although TF activity was not completely suppressed under the *in vitro* conditions, it is important to point out that inhibition by TFPI-1 is dependent on the initial generation of factor Xa and that the degree of inhibition increases over time (19). When aggressive tumor cells are progressively exposed to blood plasma components, TFPI-1 is expected to exhibit anticoagulant potency that exceeds the potency measured under tissue culture conditions. Notably, highly metastatic melanoma cells effectively counter-regulate TF activity when injected into the blood stream. Ultrastructural analysis of tumor cells that are lodged shortly after injection into the lung vascular bed show only localized fibrin deposition, but no thrombotic occlusion of the vascular lumen (58). Metastatic melanoma, similar to endothelial cells, express TFPI-1 in a glycosylphosphatidylinositol anchored form, which lends additional support to the concept that these aggressive tumor cells specifically mimic the vascular endothelial cell phenotype in regulating the TF procoagulant pathway.

Genetic profiling of tumor cell clones that differ in their metastatic and invasive potential has greatly enhanced the understanding of the phenotypic changes that distinguish these tumor cell populations. Which of the concordantly regulated genes cooperatively achieve biological function(s), such as the ability to form VM tumor cell-lined networks, remains to be determined experimentally. The data presented indicate that TFPI-2 is necessary for the formation of VM networks by aggressive melanoma cells that are cultured on three-dimensional collagen. Moreover, TFPI-2 incorporation into a collagen matrix triggers phenotypic changes in poorly aggressive tumor cells to resemble more aggressive melanoma. This finding suggests that matrix components can send signals to tumor cells to influence their VM phenotype. TFPI-2 has been shown to be mitogenic in smooth muscle cells, indicating direct cell signaling that appears to be specific for TFPI-2 relative to the closely related TFPI-1 (59). Whether direct signaling of TFPI-2 in tumor cells is a relevant mechanism that contributes to the vasculogenic switch of poorly aggressive tumor cells is an important direction for additional research.

Treating aggressive melanoma cells in three-dimensional collagen cultures with an anti-TFPI-2 antibody resulted in a decrease in the amount of endogenous MMP-2 activity with little change in the concentration of MMP-2 present in the cultures. This is an important observation because, as shown previously (7, 52), membrane type-1-MMP and MMP-2 activities are critical to melanoma VM. Whereas TFPI-2 has been shown to inhibit the activity of purified MMP-1, -2, -9, and -13, and to coprecipitate with MMPs in cell lysates of smooth muscle cells, it is unknown whether TFPI-2 regulates MMP activity in intact smooth muscle cells (28). The fact that TFPI-2 associates with MMPs in cells provides a possible explanation for the observed requirement of TFPI-2 in MMP-2 activation of aggressive melanoma

Table 2 Concentration and activity states of MMP-2 in C8161 cells on a collagen I three-dimensional matrix treated with anti-TFPI-1, -2, or TF^a

Inhibitor	MMP-2 protein concentration (% of control)	MMP-2 endogenous activity (% of control) ^b
Anti-TFPI-1	91% (4) ^c	91% (2)
Anti-TFPI-2	86% (5)	50% (3)
Anti-TF	95% (3)	91% (2)

^a Measurements performed as described under "Materials and Methods."

^b MMP-2 activity without prior activation of the MMP-2.

^c Mean of the indicated number of experiments.

cells. Direct interaction of TFPI-2 with MMP-2 may facilitate MMP-2 activation in the cellular context of aggressive melanoma cells. MMP-2 mRNA levels are also up-regulated in aggressive melanoma cells, which may ensure an excess of MMP-2 over TFPI-2 to counteract a potential subsequent inhibition of MMP-2 by TFPI-2 and, thus, increase net MMP-2 activity. However, because there are multiple pathways that link MMP-2 activation to serine proteases, TFPI-2 may have other additional targets that indirectly regulate MMP activation in the cellular environment.

The failure of aprotinin, a potent Kunitz-type inhibitor of plasmin, to reverse the effect of anti-TFPI-2 antibody indicates that inhibition of plasmin is not the mechanism by which TFPI-2 supports VM networks. Phenotypic changes induced in poorly aggressive tumor cells by the TFPI-2/K2 chimera additionally indicate that Kunitz domain 2 is not specifically contributing to this process. These data suggest a possible functional role of Kunitz domain 3 and/or the basic COOH terminus in melanoma VM. TFPI-2 binds through ionic interactions with ECM proteins (26), and the charge properties of COOH terminus of TFPI-2 may thus play a crucial role in localizing the inhibitor to relevant matrix structures. Considering the importance of MMP-2 activation in the formation of VM networks *in vitro* (7, 52), regulation of localized MMP-2 activation may define a novel function of matrix-associated TFPI-2 in VM.

The microcirculation of aggressive tumors is very complex, and depending on the window of observation, could consist of angiogenic vessels, co-opted vessels, and mosaic vessels (11–13, 37). There is also strong evidence for the existence of an intratumoral, VM tumor cell-lined ECM-rich network system capable of providing an extravascular fluid pathway, now called a fluid conducting meshwork (36, 37). The entire microcirculation in aggressive tumors appears to be comprised of a combination of these elements, resulting from destructive tumor growth and remodeling. Although the precise functional relevance of an extravascular, intratumoral pathway lined by tumor cells expressing a vascular phenotype remains unclear, there are two possibilities that should be considered. The fluid conducting meshwork might be analogous to an edematous inflammatory response, in which increased tumor pressure leads to the escape of fluid along connective tissue pathways within intratissue spaces. Alternatively, the VM tumor cell-lined meshwork might provide a nutritional exchange for aggressive tumors that might prevent necrosis.

Previous reports in melanoma and breast carcinoma using tracers and magnetic resonance imaging have indicated a physiological connection between endothelial-lined vasculature and tumor cell-lined pathways (36, 37, 40, 60, 61). The current study demonstrated an intense staining pattern for TF, TFPI-1, and TFPI-2 in aggressive human melanoma patient tumors, including along VM tumor cell-lined networks comprising the fluid-conducting meshwork. Doppler imaging of the human melanoma xenografts, using microbubbles, demonstrated pulsatile turbulent flow at the mouse-human tissue interface (with mouse endothelial-lined neovasculature) and the central region of the tumor containing VM melanoma cell-lined channel-like spaces. The overexpression of key anticoagulation pathway genes, such as TFPI-1, by aggressive melanoma cells might help to explain the possible dynamic conduction of blood through a VM tumor cell-lined meshwork. Whether this unique system functions in a lymphangiogenic manner to accommodate vascular leakage from nearby tumor vasculature remains to be elucidated. In the meantime, recent studies are demonstrating the successful targeting of endothelial cell-associated genes on aggressive tumor cells resulting in tumor destruction (38) and abrogation of the vasculogenic phenotype (8, 9).

ACKNOWLEDGMENTS

We thank Drs. H. Culver Boldt, Patricia Kirby, Robert Bhatti, and Thomas Weingeist for the human uveal melanoma histological samples, David Revak, Pablito Tejada, and Kathy Zimmerman for excellent technical assistance, and Dr. Dawn Kirschmann for RT-PCR analyses.

REFERENCES

1. Seftor, E. A., Meltzer, P. S., Schatteman, G. C., Gruman, L. M., Hess, A. R., Kirschmann, D. A., Seftor, R. E., and Hendrix, M. J. Expression of multiple molecular phenotypes by aggressive melanoma tumor cells: role in vasculogenic mimicry. *Crit. Rev. Oncol. Hematol.*, *44*: 17–27, 2002.
2. Seftor, E. A., Meltzer, P. S., Kirschmann, D. A., Pe'er, J., Maniotis, A. J., Trent, J. M., Folberg, R., and Hendrix, M. J. Molecular determinants of human uveal melanoma invasion and metastasis. *Clin. Exp. Metastasis*, *19*: 233–246, 2002.
3. Bittner, M., Meltzer, P., Chen, Y., Jiang, Y., Seftor, E., Hendrix, M., Radmacher, M., Simon, R., Yakhini, Z., Ben-Dor, A., Sampas, N., Dougherty, E., Wang, E., Marincola, F., Gooden, C., Leuders, J., Glatfelter, A., Pollack, P., Carpten, J., Gillanders, E., Leja, D., Dietrich, K., Beaudry, C., Berens, M., Alberts, D., Sondak, V., Hayward, N., and Trent, J. Molecular classification of cutaneous malignant melanoma by gene expression profiling. *Nature (Lond.)*, *406*: 536–540, 2000.
4. Maniotis, A. J., Folberg, R., Hess, A., Seftor, E. A., Gardner, L. M. G., Pe'er, J., Trent, J. M., Meltzer, P. S., and Hendrix, M. J. C. Vascular channel formation by human melanoma cells *in vivo* and *in vitro*: vasculogenic mimicry. *Am. J. Pathol.*, *155*: 739–752, 1999.
5. Hendrix, M. J. C., Seftor, E. A., Hess, A. R., and Seftor, R. E. B. Vasculogenic mimicry and tumour-cell plasticity: lessons from melanoma. *Nat. Rev. Cancer*, *3*: 411–421, 2003.
6. Folberg, R., Hendrix, M. J. C., and Maniotis, A. J. Vasculogenic mimicry and tumor angiogenesis. *Am. J. Pathol.*, *156*: 361–381, 2000.
7. Seftor, R. E. B., Seftor, E. A., Koshikawa, N., Meltzer, P. S., Gardner, L. M. G., Bilban, M., Stetler-Stevenson, W. G., Quaranta, V., and Hendrix, M. J. C. Cooperative interactions of laminin 5 γ 2 chain, matrix metalloproteinase-2, and membrane type-1-matrix/metalloproteinase are required for mimicry of embryonic vasculogenesis by aggressive melanoma. *Cancer Res.*, *61*: 6322–6327, 2001.
8. Hess, A. R., Seftor, E. A., Gardner, L. M. G., Carles-Kinch, K., Schneider, G. B., Seftor, R. E. B., Kinch, M. S., and Hendrix, M. J. C. Molecular regulation of tumor cell vasculogenic mimicry by tyrosine phosphorylation: role of epithelial cell kinase (Eck/EphA2). *Cancer Res.*, *61*: 3250–3255, 2001.
9. Hendrix, M. J. C., Seftor, E. A., Meltzer, P. S., Gardner, L. M. G., Hess, A. R., Kirschmann, D. A., Schatteman, G. C., and Seftor, R. E. B. Expression and functional significance of VE-cadherin in aggressive human melanoma cells: role in vasculogenic mimicry. *Proc. Natl. Acad. Sci. USA*, *98*: 8018–8023, 2001.
10. Hynes, R. O., Bader, B. L., and Hodivala-Dilke, K. Integrins in vascular development. *Braz. J. Med. Biol. Res.*, *32*: 501–510, 1999.
11. Carmeliet, P. Mechanisms of angiogenesis and arteriogenesis. *Nat. Med.*, *6*: 389–395, 2000.
12. Risau, W. Mechanisms of angiogenesis. *Nature (Lond.)*, *386*: 671–674, 1997.
13. Ruf, W., and Edgington, T. S. Structural biology of tissue factor, the initiator of thrombogenesis *in vivo*. *FASEB J.*, *8*: 385–390, 1994.
14. Ruf, W., and Dickinson, C. D. Allosteric regulation of the cofactor-dependent serine protease coagulation factor VIIa. *Trends Cardiovasc. Med.*, *8*: 350–356, 1998.
15. Riewald, M., and Ruf, W. Orchestration of coagulation protease signaling by tissue factor. *Trends Cardiovasc. Med.*, *12*: 149–154, 2002.
16. Huang, Z.-F., Higuchi, D., Lasky, N., and Broze, G. J., Jr. Tissue factor pathway inhibitor gene disruption produces intrauterine lethality in mice. *Blood*, *90*: 944–951, 1997.
17. Mast, A. E., Higuchi, D. A., Huang, Z. F., Warshawsky, I., Schwartz, A. L., and Broze, G. J., Jr. Glypican-3 is a binding protein on the HepG2 cell surface for tissue factor pathway inhibitor. *Biochem. J.*, *327*: 577–583, 1997.
18. Lupu, C., Goodwin, C. A., Westmuckett, A. D., Emeis, J. J., Scully, M. F., Kakkar, V. V., and Lupu, F. Tissue factor pathway inhibitor in endothelial cells colocalizes with glycolipid microdomains/caveolae. Regulatory mechanism(s) of the anticoagulant properties of the endothelium. *Arterioscler. Thromb. Vasc. Biol.*, *17*: 2964–2974, 1997.
19. Sevinsky, J. R., Rao, L. V. M., and Ruf, W. Ligand-induced protease receptor translocation into caveolae: A mechanism for regulating cell surface proteolysis of the tissue factor-dependent coagulation pathway. *J. Cell Biol.*, *133*: 293–304, 1996.
20. Mueller, B. M., and Ruf, W. Requirement for binding of catalytically active factor VIIa in tissue factor dependent experimental metastasis. *J. Clin. Invest.*, *101*: 1372–1378, 1998.
21. Carmeliet, P., Mackman, N., Moons, L., Luther, T., Gressens, P., Van Vlaenderen, I., Demunck, H., Kasper, M., Breier, G., Evrard, P., Müller, M., Risau, W., Edgington, T., and Collen, D. Role of tissue factor in embryonic blood vessel development. *Nature (Lond.)*, *383*: 73–75, 1996.
22. Contrino, J., Hair, G., Kreutzer, D. L., and Rickles, F. R. *In situ* detection of tissue factor in vascular endothelial cells: correlation with the malignant phenotype of human breast disease. *Nat. Med.*, *2*: 209–215, 1996.
23. Sprecher, C. A., Kisiel, W., Mathewes, S., and Foster, D. C. Molecular cloning, expression, and partial characterization of a second human tissue-factor-pathway inhibitor. *Proc. Natl. Acad. Sci. USA*, *91*: 3353–3357, 1994.
24. Miyagi, Y., Koshikawa, N., Yasumitsu, H., Miyagi, E., Hirahara, F., Aoki, I., Misugi, K., Umeda, M., and Miyazaki, K. cDNA cloning and mRNA expression of a serine

- proteinase inhibitor secreted by cancer cells: identification as placental protein 5 and tissue factor pathway inhibitor-2. *J. Biochem. (Tokyo)*, *116*: 939–942, 1994.
25. Rao, C. N., Reddy, P., Liu, Y. Y., O'Toole, E., Reeder, D., Foster, D. C., Kisiel, W., and Woodley, D. T. Extracellular matrix-associated serine protease inhibitors (*M*₁, 33,000, 31,000, and 27,000) are single-gene products with differential glycosylation: cDNA cloning of the 33-kDa inhibitor reveals its identity to tissue factor pathway inhibitor-2. *Arch. Biochem. Biophys.*, *335*: 82–92, 1996.
 26. Liu, Y. Y., Stack, S. M., Lakka, S. S., Khan, A. J., Woodley, D. T., Rao, J. S., and Rao, C. N. Matrix localization of tissue factor pathway inhibitor-2/matrix-associated serine protease inhibitor (TFPI-2/MSPI) involves arginine-mediated ionic interactions with heparin and dermatan sulfate: heparin accelerates the activity of TFPI-2/MSPI toward plasmin. *Arch. Biochem. Biophys.*, *370*: 112–118, 1999.
 27. Petersen, L. C., Sprecher, C. A., Foster, D. C., Blumberg, H., Hamamoto, T., and Kisiel, W. Inhibitory properties of a novel human Kunitz-type protease inhibitor homologous to tissue factor pathway inhibitor. *Biochemistry*, *35*: 266–272, 1996.
 28. Herman, M., Sukhova, G. K., Kisiel, W., Foster, D., Kehry, M., Libby, P., and Schonbeck, U. Tissue factor pathway inhibitor-2 is a novel inhibitor of matrix metalloproteinases with implications for atherosclerosis. *J. Clin. Invest.*, *107*: 1117–1126, 2001.
 29. Izumi, H., Takahashi, C., Oh, J., and Noda, M. Tissue factor pathway inhibitor-2 suppresses the production of active matrix metalloproteinase-2 and is down-regulated in cells harboring activated *ras* oncogenes. *FEBS Lett.*, *481*: 31–36, 2000.
 30. Jin, M., Udagawa, K., Miyagi, E., Nakazawa, T., Hirahara, F., Yasumitsu, H., Miyazaki, K., Nagashima, Y., Aoki, I., and Miyagi, Y. Expression of serine proteinase inhibitor PP5/TFPI-2/MSPI decreases the invasive potential of human choriocarcinoma cells *in vitro* and *in vivo*. *Gynecol. Oncol.*, *83*: 325–333, 2001.
 31. Konduri, S. D., Tasiou, A., Chandrasekar, N., Nicolson, G. L., and Rao, J. S. Role of tissue factor pathway inhibitor-2 (TFPI-2) in amelanotic melanoma (C-32) invasion. *Clin. Exp. Metastasis*, *18*: 303–308, 2000.
 32. Rao, C. N., Reddy, P., Reeder, D. J., Liu, Y., Stack, S. M., Kisiel, W., and Woodley, D. T. Prokaryotic expression, purification, and reconstitution of biological activities (antiprotease, antitumor, and heparin-binding) for tissue factor pathway inhibitor-2. *Biochem. Biophys. Res. Commun.*, *276*: 1286–1294, 2000.
 33. Neaud, V., Hisaka, T., Monvoisin, A., Bedin, C., Balabaud, C., Foster, D., Desmouliere, A., Kisiel, W., and Rosenbaum, J. Paradoxical pro-invasive effect of the serine proteinase inhibitor tissue factor pathway inhibitor-2 on human hepatocellular carcinoma cells. *J. Biol. Chem.*, *275*: 35565–35569, 2000.
 34. Blind, R., Vogt, F., Lamby, D., Zeiffer, U., Krott, N., Hilger-Eversheim, K., Hanrath, P., vom, D. J., and Bosserhoff, A. K. Characterization of differential gene expression in quiescent and invasive human arterial smooth muscle cells. *J. Vasc. Res.*, *39*: 340–352, 2002.
 35. Iino, M., Foster, D. C., and Kisiel, W. Quantification and characterization of human endothelial cell-derived tissue factor pathway inhibitor-2. *Arterioscler. Thromb. Vasc. Biol.*, *18*: 40–46, 1998.
 36. Clarijs, R., Otte-Holler, I., Ruiter, D. J., and de Waal, R. M. Presence of a fluid-conducting meshwork in xenografted cutaneous and primary human uveal melanoma. *Invest. Ophthalmol. Vis. Sci.*, *43*: 912–918, 2002.
 37. Maniotis, A. J., Chen, X., Garcia, C., DeChristopher, P. J., Wu, D., Pe'er, J., and Folberg, R. Control of melanoma morphogenesis, endothelial survival, and perfusion by extracellular matrix. *Lab. Invest.*, *82*: 1031–1043, 2002.
 38. Liu, C., Huang, H., Donate, F., Dickinson, C., Santucci, R., El Sheikh, A., Vessella, R., and Edgington, T. S. Prostate-specific membrane antigen directed selective thrombotic infarction of tumors. *Cancer Res.*, *62*: 5470–5475, 2002.
 39. Shirakawa, K., Kobayashi, H., Heike, Y., Kawamoto, S., Brechbiel, M. W., Kasumi, F., Iwanaga, T., Konishi, F., Terada, M., and Wakasugi, H. Hemodynamics in vasculogenic mimicry and angiogenesis of inflammatory breast cancer xenograft. *Cancer Res.*, *62*: 560–566, 2002.
 40. Kobayashi, H., Shirakawa, K., Kawamoto, S., Saga, T., Sato, N., Hiraga, A., Watanabe, I., Heike, Y., Togashi, K., Konishi, J., Brechbiel, M. W., and Wakasugi, H. Rapid accumulation and internalization of radiolabeled hereceptin in an inflammatory breast cancer xenograft with vasculogenic mimicry predicted by the contrast-enhanced dynamic MRI with the macromolecular contrast agent G6-(1B4M-Gd)₂₅₆. *Cancer Res.*, *62*: 860–866, 2002.
 41. Ruf, W. Factor VIIa residue Arg²⁹⁰ is required for efficient activation of the macromolecular substrate factor X. *Biochemistry*, *33*: 11631–11636, 1994.
 42. Dickinson, C. D., and Ruf, W. Active site modification of factor VIIa affects interactions of the protease domain with tissue factor. *J. Biol. Chem.*, *272*: 19875–19879, 1997.
 43. Fischer, E. G., Riewald, M., Huang, H. Y., Miyagi, Y., Kubota, Y., Mueller, B. M., and Ruf, W. Tumor cell adhesion and migration supported by interaction of a receptor-protease complex with its inhibitor. *J. Clin. Invest.*, *104*: 1213–1221, 1999.
 44. Ott, I., Miyagi, Y., Miyazaki, K., Heeb, M. J., Mueller, B. M., Rao, L. V. M., and Ruf, W. Reversible regulation of tissue factor-induced coagulation by glycosyl phosphatidylinositol-anchored tissue factor pathway inhibitor. *Arterioscler. Thromb. Vasc. Biol.*, *20*: 874–882, 2000.
 45. Ruf, W., and Edgington, T. S. An anti-tissue factor monoclonal antibody which inhibits TF:VIIa complex is a potent anticoagulant in plasma. *Thromb. Haemost.*, *66*: 529–533, 1991.
 46. Ruf, W., Rehemtulla, A., and Edgington, T. S. Antibody mapping of tissue factor implicates two different exon-encoded regions in function. *Biochem. J.*, *278*: 729–733, 1991.
 47. Wun, T.-C., Kretzmer, K. K., Girard, T. J., Miletich, J. P., and Broze, G. J. Cloning and characterization of a cDNA coding for the lipoprotein-associated coagulation inhibitor shows that it consists of three tandem Kunitz-type inhibitory domains. *J. Biol. Chem.*, *263*: 6001–6004, 1988.
 48. Stone, M. J., Ruf, W., Miles, D. J., Edgington, T. S., and Wright, P. E. Recombinant soluble human tissue factor secreted by *Saccharomyces cerevisiae* and refolded from *Escherichia coli* inclusion bodies: glycosylation of mutants, activity, and physical characterization. *Biochem. J.*, *310*: 605–614, 1995.
 49. Shoji, M., Hancock, W. W., Abe, K., Micko, C., Casper, K. A., Baine, R. M., Wilcox, J. N., Danave, I., Dillehay, D. L., Matthews, E., Contrino, J., Morrissey, J. H., Gordon, S., Edgington, T. S., Kudryk, B., Kreutzer, D. L., and Rickles, F. R. Activation of coagulation and angiogenesis in cancer. Immunohistochemical localization *in situ* of clotting proteins and vascular endothelial growth factor in human cancer. *Am. J. Pathol.*, *152*: 399–411, 1998.
 50. Kamei, S., Petersen, L. C., Sprecher, C. A., Foster, D. C., and Kisiel, W. Inhibitory properties of human recombinant Arg²⁴→Gln type-2 tissue factor pathway inhibitor (R24Q TFPI-2). *Thromb. Res.*, *94*: 147–152, 1999.
 51. Bell, S. E., Mavila, A., Salazar, R., Bayless, K. J., Kanagala, S., Maxwell, S. A., and Davis, G. E. Differential gene expression during capillary morphogenesis in 3D collagen matrices: regulated expression of genes involved in basement membrane matrix assembly, cell cycle progression, cellular differentiation and G-protein signaling. *J. Cell Sci.*, *114*: 2755–2773, 2001.
 52. Seftor, R. E., Seftor, E. A., Kirschmann, D. A., and Hendrix, M. J. Targeting the tumor microenvironment with chemically modified tetracyclines: inhibition of laminin 5 [γ]2 chain promigratory fragments and vasculogenic mimicry. *Mol. Cancer Ther.*, *1*: 1173–1179, 2002.
 53. Shirakawa, K., Tsuda, H., Heike, Y., Kato, K., Asada, R., Inomata, M., Sasaki, H., Kasumi, F., Yoshimoto, M., Iwanaga, T., Konishi, F., Terada, M., and Wakasugi, H. Absence of endothelial cells, central necrosis, and fibrosis are associated with aggressive inflammatory breast cancer. *Cancer Res.*, *61*: 445–451, 2001.
 54. Pezzella, F. Evidence for novel non-angiogenic pathway in breast-cancer metastasis. *Lancet*, *355*: 1787–1788, 2000.
 55. Sood, A. K., Seftor, E. A., Fletcher, M. S., Gardner, L. M. G., Heidger, P. M., Buller, R. E., Seftor, R. E. B., and Hendrix, M. J. C. Molecular determinants of ovarian cancer plasticity. *Am. J. Pathol.*, *158*: 1279–1288, 2001.
 56. Sharma, N., Seftor, R. E. B., Seftor, E. A., Gruman, L. M., Heidger, P. M., Jr., Cohen, M. B., Lubaroff, D. M., and Hendrix, M. J. C. Prostatic tumor cell plasticity involves cooperative interactions of distinct phenotypic subpopulations: role in vasculogenic mimicry. *Prostate*, *50*: 189–201, 2002.
 57. Passalidou, E., Trivella, M., Singh, N., Ferguson, M., Hu, J., Cesario, A., Granone, P., Nicholson, A. G., Goldstraw, P., Ratcliffe, C., Tetlow, M., Leigh, I., Harris, A. L., Gatter, K. C., and Pezzella, F. Vascular phenotype in angiogenic and non-angiogenic lung non-small cell carcinomas. *Br. J. Cancer*, *86*: 244–249, 2002.
 58. Ruf, W., and Mueller, B. M. Tissue factor in cancer angiogenesis and metastasis. *Curr. Opin. Hematol.*, *3*: 379–384, 1996.
 59. Shinoda, E., Yui, Y., Hattori, R., Tanaka, M., Inoue, R., Aoyama, T., Takimoto, Y., Mitsui, Y., Miyahara, K., Shizuta, Y., and Sasayama, S. Tissue factor pathway inhibitor-2 is a novel mitogen for vascular smooth muscle cells. *J. Biol. Chem.*, *274*: 5379–5384, 1999.
 60. Potgens, A. J., van Altena, M. C., Lubsen, N. H., Ruiter, D. J., and de Waal, R. M. Analysis of the tumor vasculature and metastatic behavior of xenografts of human melanoma cell lines transfected with vascular permeability factor. *Am. J. Pathol.*, *148*: 1203–1217, 1996.
 61. Hendrix, M. J. C., Seftor, E. A., Meltzer, P. S., Hess, A. R., Gruman, L. M., Nickoloff, B. J., Miele, L., Sheriff, D. D., Schattman, G. C., Bourdon, M. A., and Seftor, R. E. B. The plasticity of aggressive melanoma tumor cells: recapitulation of an embryonic stem cell program. *Rec. Adv. Res. Updates*, *3*: 191–200, 2002.